

Economic Objective Optimization for Thermal, Solar Photovoltaic and Variable Speed Pumped Storage Hydro Hybrid Power Systems

www.rericjournal.ait.ac.th

Tan Minh Phan*, , My-Ha Le*, Thang Trung Nguyen, and Minh Phuc Duong, 1

ARTICLE INFO

Article history:
Received 18 July 2025
Received in revised form
07 October 2025
Accepted 27 October 2025

Keywords:
Equilibrium optimizer
Hybrid power systems
Pumped storage
hydropower plants
Secretary bird optimization
algorithm
Solar photovoltaic power
plants

ABSTRACT

The study applies the equilibrium optimizer (EO) and the secretary bird optimization algorithm (SBOA) to minimize the total electricity generation fossil fuel costs of thermal power plants (ThPPs) in hybrid power systems with solar photovoltaic power plants (SoPPs) and pumped storage hydropower plants (PuHPs) for one operating day. Two systems are employed: System 1 has two ThPPs and one SoPP, and System 2 is expanded by integrating one more PuHP into System 1. The generation of the SoPP is calculated using solar radiation from a specific location in Vietnam; meanwhile, the generation of ThPPs and the pumping power and generation of the PuHP are optimally determined by EO and SBOA. The pumping power and generation of the PuHP are supposed to be continuous. System 2 is run for two cases: Case 1- no running pumps, and Case 2running pumps. As a result, EO can reach smaller costs than SBOA for the two systems. System 1 costs the most, \$9,155,384, whereas Case 2 of System 2 costs the least, \$9,006,450. System 2 can reach a smaller cost than System 1 by \$148,934, about 1.63%. For System 2, the total cost of Case 2 is smaller than that of Case 1 by \$81,025 per day, about 0.9%. The results indicate that the optimal operation of pumps in PuHPs can contribute to a high-cost reduction for ThPPs in hybrid power systems.

1. INTRODUCTION

The energy storage system is one of the valuable solutions that brings many significant benefits to the operation and development of modern power systems [1]. It helps to improve the efficiency of renewable energy plants and reduce the ThPPs [2]. Firstly, it improved the grid's stability by balancing the power load and minimizing local line overloads or interruptions. In addition, this storage system also overcomes the disadvantages of renewable energy sources, such as the SoPPs and wind power, by storing excess electricity when the line is overloaded and supplying it back when the line is underloaded. As a result, the electricity grid system does not have to invest in a new transmission and generation infrastructure, which is time-consuming and costly [3]. Secondly, this system improves system operating efficiency through voltage regulation and power quality control, leading to a flexible power supply that quickly responds to important loads or

DOI: https://doi.org/10.64289/iej.25.0412.4847963

¹Corresponding author: Tel: +84354652160

Email: duongphucminh@tdtu.edu.vn

emergencies. Finally, to develop sustainable energy use, this system reduces greenhouse gas emissions and promotes sustainable energy transition. However, operating these systems to bring the best efficiency and satisfy technical constraints is an important issue that needs to be solved. In this paper, PuHPs are applied as energy storage units to reduce the total fuel cost of ThPPs in power systems.

Metaheuristic optimization algorithms applied to solve the operation problems for hybrid power systems combining PuHPs, renewable energy, and ThPPs with various constraints [4]–[9]. The above studies apply PuHPs models with the relationship between electric power and water flow expressed through linear formulas in quadratic functions. Constraints related to the operation of PuHPs, such as generation and pumping capacity limits, discharge and pumping flow limits, water balance constraints in the reservoir over time, and constraints on the final reservoir volume equal to the initial reservoir volume, have been considered. Study [4] applies the Jellyfish Search Algorithm (JSA) to the optimal operation problem of a hybrid system combining PuHPs, wind power, ThPPs, and SoPPs. The objective is to optimize the operating cost. EO [5], Slime Mould Algorithm (SMA) [5], and Improved Slime Mould Algorithm (ISMA) [5] are used for the hybrid system consisting of cascade hydro, thermal, PuHPs, wind, and SoPPs. Differential Evolution (DE) algorithm is used to find the optimal solution in the study [6]. The study considers two cases: a system consisting of only ThPPs and a system with

^{*} Faculty of Electrical and Electronics Engineering, Ho Chi Minh City University of Technology and Education, Ho Chi Minh City, Vietnam.

[^] Power System Optimization Research Group, Faculty of Electrical and Electronics Engineering, Ton Duc Thang University, Ho Chi Minh City, Vietnam.

additional PuHPs to analyze the benefits. A quadratic function models the fuel cost function of ThPPs. The transmission line losses are calculated using the Newton-Raphson power flow method. The constraints of the problem are handled through the penalty method. The results obtained from DE are compared with other algorithms in the literature [7]. Self-organizing Migrating Algorithm (SOMA) [8] and improved selforganizing migration algorithm (ISOMA) [9] were applied and proposed to find optimal storage and discharge of the PuHP and the optimal generation of ThPPs in power systems. Salp Swarm Algorithm (SSA) and Dragonfly algorithm (DA) were applied to find optimal solutions, but they could not find solutions of the same quality as SOMA and ISOMA. Mixed Integer Linear Programming model was applied to operate a power system with a 976 MW PuHP to maximize the total profit [10]. A standalone combined system with wind turbines, SoPPs, biomass units, and PuHP was optimally operated [11]. Another standalone system with PuHPs and wind turbines supplied power to an extensive power system. The economic risk of the standalone system was analyzed to conclude whether it should be installed or not [12]. The study [13] assumes that a conventional hydropower plant is converted to PuHP to improve efficiency. A PuHP with variable pump speeds was integrated into a system with SoPPs and wind turbines [14]. A small-capacity PuHP was integrated into microgrids with battery energy storage systems (BESS), supplied by renewable energies, considering the uncertainty of renewable power sources [15]. Three targets, including economy, technique, and environment, were evaluated in one off-grid combined power system with solar array tracker, BESS, and PuHP [16]. The configuration of a combined system using PuHP, BESS, solar arrays, biomass units, and wind turbines was determined optimally by using Heap Optimization Algorithm (HOA) [17], the non-dominated sorting whale optimization algorithm (NSWOA), and nondominated sorting genetic algorithm-II (NSGA-II) [18]. The electric market was considered when running PuHP in a combined system with PuHP and renewable power sources [19]. By using a modified bat algorithm, PuHP and other renewable power plants were operated optimally, leading to a huge benefit from the generation process [20]. A power system in Raglan, Canada, was operated optimally to improve the sustainability of energy via the remote control of wind turbines and PuHP [21]. A hybrid renewable energy system was designed for a microgrid in Dakhla, Morocco, featuring wind turbines (WTs), BESS, SoPPs, and diesel-based generators [22]. The impact of wind speed, solar radiation, and diesel fuel costs on the grid's total cost and energy price was investigated. As a result, the best grid cost and energy price per kWh were \$74,327 and \$0.0917. Two hybrid systems for a microgrid in El Kharga Oasis, Egypt, were designed [23]. The first system included PVSS, BESS, DGs, and WTs, costing \$286,874 for the whole system and \$0.2309 for each kWh. The second system, which excluded WTs, had a total cost of \$322,674 and an energy price per kWh of \$0.2597. The cost and energy price of three systems in the Farafra region of Egypt were examined [24]. Those of the first system with all components were \$187,181 and \$0.213 per kWh. Those of the second system were \$214,530 and \$0.2452 per kWh, while those of the third system, which excluded SPs, were \$603,026 and \$1.81 per kWh.

In general, the studies above have shown good results in cost reduction and profit enhancement after running PuHPs in power systems with and without renewable power sources. The studies applied or developed a modified version of existing algorithms to get better results. They had significant contributions to power systems. However, they did not prove the real performance of PuHPs when considering the variable pump speed of PuHPs. The PuHPs have two operation modes, including electricity generation and water storage. When the inflows are significant over the scheduled time, a huge amount of energy can be produced by the PuHPs, even if we do not care if the water storage operation is optimal. In general, the efficiency of pumps was considered to be 0.75, so if the operation of pumps is not effective, the water storage can lead to a loss of energy. The conventional hydropower plants without water storage functions can produce high energy for power systems, reducing the high power for ThPPs. Clearly, the research gap regarding the neglect of the pumping effectiveness of the PuHPs was seen in the previous studies. So, their contributions to the power system are not highly accurate. The big problem is indicated and proven in the study. In the study, EO [25] and SBOA [26] are applied for two systems, in which the second system comprises one SoPPs, two ThPPs, and one PuHP. The second system is simulated for two cases: Case 1: The PuHP does not run pumps, and Case 2: The PuHP can run pumps. In Case 1, the system is solved to find the optimal power of the PuHP and the optimal generation of the two ThPPs. In Case 2, the system is solved to find optimal pump power and generation of the PuHP and optimal generation of the two ThPPs. In the two cases, the inflows to the PuHP are the same, indicating the effectiveness of pump operations. The comparison of the two can solve the research gaps of the previous studies. In addition, EO and SBOA were applied in early 2025 for engineering problems, and they were proven to be more effective than other popular and well-known metaheuristic algorithms [27], [28]. So, the two algorithms are selected as optimization tools for the study. The novelty of the study is summarized as follows:

- Apply EO and SBOA to the problem of optimal scheduling of thermal-solar-pumped storage power plants.
- The variable pump speed of PuHP is considered in the study.

After running EO and SBOA for simulation cases, the results are compared and analyzed to show the following contributions:

 The applied EO and SBOA are powerful algorithms for the problem. They can get a 100% success rate for simulation cases. So they

- will be able to solve more complex problems in electrical engineering.
- The total load demand can be supplied, and the total costs of ThPPs can be reduced based on the optimal operation of pumps.

2. PROBLEM FORMULAR

2.1 Objective Function

This study investigates how PuHPs contribute to reducing the cost of ThPPs. A typical power system that includes various power plants, such as N_{ThPP} , ThPPs, N_{PuHP} , PuHPs, and N_{SoPP} SoPPs, is considered. The power from all power plants will be determined so that the objective function of the system is to reduce the fuel cost (FC) from ThPPs [4]. Its formulation is given by:

$$FC = \sum_{t=1}^{24} \sum_{k=1}^{N_{ThPP}} \left(a_k + b_k \times ThPP_{k,t}^{Ge} + c_k \times (ThPP_{k,t}^{Ge})^2 \right)$$
 (1)

where, a_k , b_k , and c_k are cost parameters of the *kth* ThPP; and $ThPP_{k,t}^{Ge}$ is the power output of the *kth* ThPP at the *tth* hour.

2.2 Constraints

2.2.1 Power balance constraint

The constraint is a fundamental requirement for ensuring the stability of power systems. The total power generated by all power plants must match the total load demand, including any losses in the transmission lines as assigned in Equation (2).

$$\sum_{k=1}^{N_{ThPP}} (ThPP_{k,t}^{Ge}) + \sum_{m=1}^{N_{SoPP}} (SoPP_{m,t}^{Ge}) + \sum_{l=1}^{N_{PuHP}} (1 - KNOP_{l,t}) PuHP_{l,t}^{Ge})$$

$$- \sum_{l=1}^{N_{PuHP}} (KNOP_{l,t} \cdot PuHP_{l,t}^{Pu}) - Load_t - Loss_t$$
(2)

where, $PuHP_{l,t}^{Ge}$, $PuHP_{l,t}^{Pu}$ and $KNOP_{l,t}$ are obtained by [15].

$$PuHP_{l,t}^{Ge} = g \times H_{l,t} \times \rho \times Q_{l,t}^{Ge} \times \eta_{Ge}$$
 (3)

$$PuHP_{l,t}^{Pu} = \frac{g \times H_{l,t} \times \rho \times Q_{l,t}^{Pu}}{\eta_{Pu}}$$
 (4)

$$KNOP_{l,t} = \begin{cases} 1, & \text{for pump status} \\ 0, & \text{for generation status} \end{cases}$$
 (5)

In constraint (2), the first three terms are from the generation sides; meanwhile, the last three terms are from the consumed side. Namely, $\sum_{k=1}^{N_{ThPP}} (ThPP_{k,t}^{Ge})$ is the total generation of all N_{ThPP} ThPPs at the *tth* hour.

 $\textstyle \sum_{l=1}^{N_{PuHP}} \left(\left(1-KNOP_{l,t}\right) PuHP_{l,t}^{Ge} \right)$ the total generation of all N_{PuHP} PuHPs at the tth hour in case that the operating status is generation (i.e., $KNOP_{l,t}$ = 0); $\sum_{m=1}^{N_{SOPP}} (SoPP_{m,t}^{Ge})$ is the total generation of all N_{SOPP} SoPPs at the tth hour. $\sum_{l=1}^{N_{PuHP}} \left(KNOP_{l,t} \cdot PuHP_{l,t}^{Pu}\right)$ is the total consumed power of the pumps of all PuHPs in case that the operating status is pump (i.e., $KNOP_{l,t} = 1$). $Load_t$ and $Loss_t$ are the total demand of all loads and losses on all transmission lines at the tth hour. However, the study neglects the losses on all transmission lines. In addition, symbols in constraint (2) are explained as follows: N_{ThPP} , N_{PuHP} and N_{SoPP} are the numbers of ThPPs, PuHPs and SoPPs. $KNOP_{l,t}$ is the operation mode of the *lth PuHP* at the *tth* hour; $PuHP_{l,t}^{Ge}$ is the power output of the lth PuHP in the generation process at tth hour. $PuHP_{l,t}^{Pu}$ is the power demand of the lth PuHP in the pumping process at the *tth* hour; $SoPP_{m\,t}^{Ge}$ is the power output of the *mth SoPP* at the *tth* hour.

Equation (3) and Equation (4) are used to determine the generation and the pump power of the lth PuHP at the *tth* hour if the operating status is generation and pump, respectively, in which Eq. (5) is employed to determine the operating status. In the study, the operating status $KNOP_{l,t}$ is a very important parameter that results in the minimum cost of all ThPPs in the power system. If the parameter is selected to be 0 (i.e., generation mode), the discharge parameter $Q_{l,t}^{Ge}$ will be produced and the value of $PuHP_{l,t}^{Ge}$ will be determined by using Equation (3). For another case, if $KNOP_{l,t}$ is selected to be 1 (i.e., pump mode), the pumped flow $Q_{l,t}^{Pu}$ will be produced and the value of $PuHP_{l.t.}^{Pu}$ will be calculated by using Equation (4). So, the PuHPs have three key parameters, including $KNOP_{l,t}$, $Q_{l,t}^{Ge}$ and $Q_{l,t}^{Pu}$, which are optimally determined by the applied metaheuristic algorithms EO and SBOA. In the two equations, $H_{l,t}$ is the net head in (m). g is the gravity acceleration in (m/s²). ρ is the water density in (kg/m³). η_{Ge} and η_{Pu} are the generation and pump efficiency. $Q_{l,t}^{Ge}$ and $Q_{l,t}^{Pu}$ are the discharge for generating and storing for pumping.

2.2.2 Generation power constraint

Power plants must operate within a defined range of generation, from lower to upper limits, to meet economic and technical demands effectively.

$$ThPP_k^{Ge,min} \le ThPP_k^{Ge} \le ThPP_k^{Ge,max} \tag{6}$$

$$SoPP_{m}^{Ge,min} \le SoPP_{m}^{Ge} \le SoPP_{m}^{Ge,max}$$
 (7)

$$PuHP_{l}^{Gen,min} \leq PuHP_{l}^{Gen} \leq PuHP_{l}^{Gen,max} \tag{8}$$

where, $ThPP_k^{Ge,min}$, $SoPP_m^{Ge,min}$, and $PuHP_l^{Gen,min}$ are lower power output of power plants; and $ThPP_k^{Ge,max}$, $SoPP_m^{Ge,max}$, and $PuHP_l^{Gen,max}$ are upper power output of power plants.

2.2.3 Hydraulic constraints

Reservoir and discharge limitations: Upper reservoirs of PuHPs, often referred to as hydropower plant reservoirs, play a crucial role in ensuring safe and efficient operation. These reservoirs have defined limits for both water storage and discharge. The storage limits are vital for maintaining the safety and integrity of the reservoir, while the discharge limits protect the turbines and generators from potential damage. The water volume in the reservoir and the water discharged through the turbines during each operational hour must comply with established guidelines consistently. Their limitations are given by:

$$V_l^{min} \le V_{l,t} \le V_l^{max} \tag{9}$$

$$Q_l^{min} \le Q_{l,t} \le Q_l^{max} \tag{10}$$

where, V_l^{min} , V_l^{max} , and $V_{l,t}$ are the lower, upper and operating reservoir volumes; Q_l^{min} , Q_l^{max} , and $Q_{l,t}$ are the lower, upper and operating water discharge.

Volume constraint at the end: Before creating a daily generation plan for a hydropower plant, it is essential to know the water volume available in the upper reservoir. This volume is a predefined input parameter. Along with the inflows into the reservoir, this information is used to estimate the energy that will be generated over the day. At the end of the last hour of the day, the reservoir volume is recalculated. This final volume, which is also a predefined parameter, must meet specific criteria as per the following equation

$$V_{l,0} = V_{l,24} \tag{11}$$

3. THE IMPLEMENTATION OF APPLIED ALGORITHMS

3.1 Equilibrium Optimizer

The EO is the meta-heuristic algorithm proposed based on the balance principle of mass in the control volume. In fact, EO is actually a physics-based meta-heuristic algorithm; however, the whole optimization process of EO while dealing with a given optimization problem is identical to other meta-heuristic algorithms except for its update procedure to the new solutions.

At first, EO also executes the generation of a set of solutions at the beginning of its optimization process using the following models

$$S_i = S_i + \delta \times \left(S_i^{max} - S_i^{min}\right); i = 1, 2 \dots, Ps$$
 (12)

$$F_i = OF(S_i) \tag{13}$$

where, S_i is the current solution ith; δ is a random value within zero and one; S_i^{max} and S_i^{min} are the maximum and minimum boundaries of the solution ith; Ps is the population size; F_i is the fitness value of the solution S_i ; OF is the main objective function featured by the given optimization problem.

After determining the fitness values for all solutions using Equations (12) and (13), the elite solutions are identified. This selection is based on the four best fitness values from the top four solutions. Additionally, the average best fitness is determined by calculating the mean of these top four solutions, as presented in Equation (14).

$$S^{elt} \in \left[S_{top1}; S_{top2}; S_{top3}; S_{top4}; S_{avg} \right] \tag{14}$$

where S^{elt} is the elite solution that is randomly selected from the elite group; S_{top1} , S_{top2} , S_{top3} , S_{top4} , and S_{avg} are the top four-best solutions and the average best solution is determined by the top four-best solutions.

When the S^{elt} is identified, the main procedure of the update process is executed using the following mathematical models

$$S_i^{new} = S^{elt} + (S_i - S^{elt}) \times \gamma + \frac{Grt}{rnd \times CV} \times (1 - \gamma)$$
(15)

$$Grt = Grt_0 \times \gamma \tag{16}$$

$$Grt_0 = AF \times (S^{elt} - rand \times S_k)$$
 (17)

$$AF = \begin{cases} 0.5 \times rnd_1 & rnd_2 \ge RF \\ 0 & rnd_2 < RF \end{cases} \tag{18}$$

$$\gamma = \alpha_1 \times sign(rnd - 0.5) \times (e^{-rnd \times \varepsilon} - 1)$$
 (19)

$$\varepsilon = \left(1 - \frac{IT^{Pre}}{IT^{Max}}\right)^{(\alpha_2 \times \frac{IT^{Pre}}{IT^{Max}})} \tag{20}$$

where, S_i^{new} is the *ith* new solution, γ is the exponential element; Grt is generating rate; the Grt_0 the standard generating rate; AF is the amplifying coefficient; RF reference factor; ε is the dependent factor; rnd is the random number within zero and one, CV is the constant volume; IT^{Pre} and IT^{Max} are the present and maximum index of iteration; α_1 and α_2 are t the two constant factors that manipulate the exploration and exploitation capability.

Figure 1 presents the application of EO for a general optimization problem.

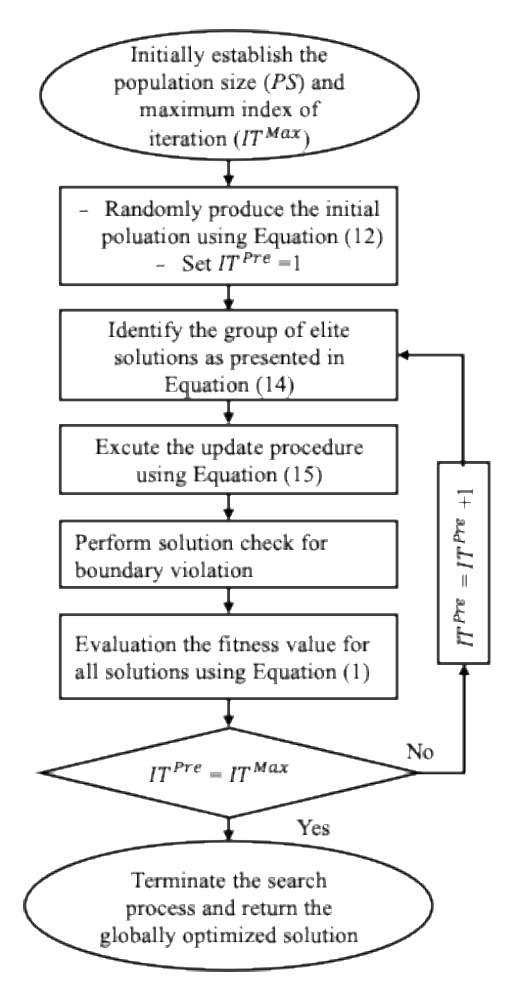


Fig. 1. The application of EO for a general optimization problem.

3.2 Secretary Bird Optimization Algorithm

The SBOA is a metaheuristic algorithm inspired by mimicking the effective hunting behaviors of the secretary bird. By applying these strategies, SBOA provides an impressive search performance compared to previous methods in solving optimization problems, including theoretical and practical ones. Unlike EO, SBOA is classified as a nature-inspired meta-heuristic algorithm. However, SBOA shares the same structure of the optimization process, similar to EO and others, such as the initialization, the first evaluation of randomly produced solutions, and others; however, the main feature that differentiates SBOA from EO and many others is its update procedure, which will be described using particular mathematical expressions as follows:

3.2.1 Exploration phase

In this phase, the update procedure is broken down into three stages corresponding to the current index of iterations as described below:

• Stage 1:
$$IT^{Pre} \le \frac{1}{3}IT^{Max}$$

$$S_i^{new,s1} = S_i + \sigma_1 \times (S_{rs1} - S_{rs2});$$

$$i = 1,2..., Ps$$
(21)

where $S_i^{new,s1}$ is the new solution *ith* updated in phase 1, σ_1 is a random within zero and one, S_{rs1} and S_{rs2} are random selected solutions among the current state of population.

• Stage 2:
$$\frac{1}{3}IT^{Max} < IT^{Pre} \le \frac{2}{3}IT^{Max}$$

$$S_i^{new,s2} = S_{best} + exp\left(\left(\frac{IT^{Pre}}{IT^{Max}}\right)^4\right) \times (S_{best} - S_i) \times (\sigma_2 - 0.5);$$

$$i = 1, 2 \dots, Ps$$
(22)

where, $S_i^{new,s3}$ is the new solution *i* updated in Stage 3; *LV* the value resulted by Levy flight distribution.

3.2.2 Exploitation stage

In this exploitation phase, the update process for all the solutions is conducted using the following expression:

$$S_i^{new} = \begin{cases} S_{best} + (2 \times \sigma_2 - 1) \left(1 - \frac{IT^{Pre}}{IT^{Max}} \right)^2 X_i, & \text{if rand } < 0.5 \\ S_i + \sigma_3 \times (S_{rs3} - \omega \times X_i), & \text{otherwise} \end{cases}$$
 (24)

where, σ_3 a random value between zero and one; S_{rs3} is the random selected solution from the current state of population.

Figure 2 presents the application of SBOA for a general optimization problem.

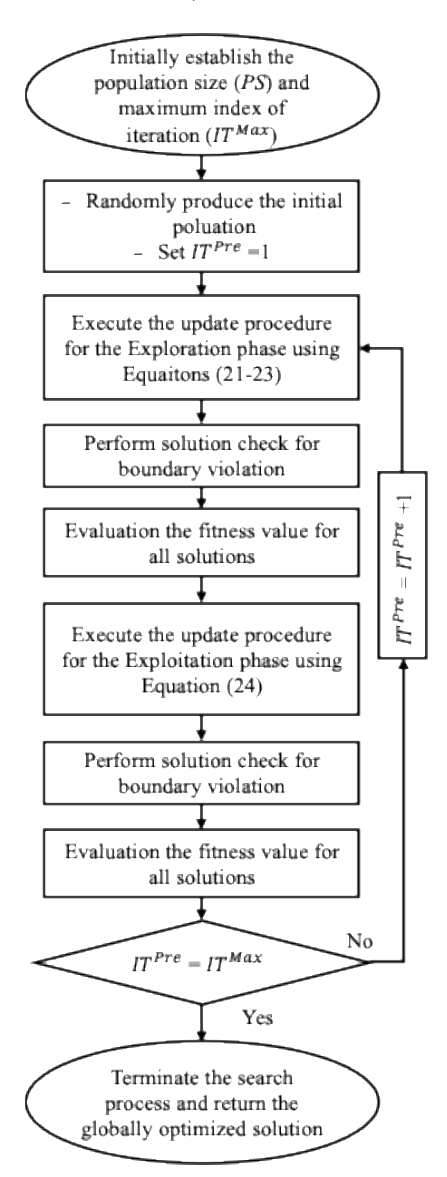


Fig. 2. The application of SBOA for a general optimization problem.

3.3 Fitness Function Calculation

3.3.1 Decision variables

Decision variables comprise the operating status $KNOP_{l,t}$, discharge $Q_{l,t}^{Ge}$ and pumped flow $Q_{l,t}^{Pu}$ of the PuHPs, and the generation of all ThPPs $ThPP_{k,t}^{Ge}$ excluding the first ThPP (i.e., $k \neq 1$). So, the set of the variables is included in the solution of EO and SBOA for initial generation before the iterative algorithm and for new update in the iterative algorithm. Namely, the decision variable set (DVS) is as follows:

$$DVS = [KNOP_{l,t}, Q_{l,t}^{Ge}, Q_{l,t}^{Pu}, ThPP_{k,t}^{Ge}]$$
 (25)

The decision variable set is updated in each iteration by using Equation (15) for EO and Equations (21) to (24) for SBOA.

3.3.2 Dependent variables

In contrast to decision variables, dependent variables are obtained by using available equations shown in Section 2. After having three decision variables $KNOP_{l,t}$, $Q_{l,t}^{Ge}$, $Q_{l,t}^{Pu}$, the pumping power or generation of the PuHPs is obtained by using Equations (3) to (4). $SoPP_{m,t}^{Ge}$ is looked

up by using the predetermined location; meanwhile, the load demand $Load_t$ is the input data. Thus, constraint (2) is converted into the constraint of the first ThPP in the system (i.e., $ThPP_{1,t}^{Ge}$).

3.3.3 Fitness function

The fitness function of the problem is determined as follows:

$$\begin{split} F_k &= FC + F_{pe} \times \left(\Delta P u H P_{l,t}^{Ge} + \Delta P u H P_{l,t}^{Pu} \right. \\ &+ \Delta T h P P_{l,t}^{Ge} + \Delta V_{l,t} \right) \end{split} \tag{26}$$

where, F_{pe} is the penalty coefficient of the violated dependent variables. $\Delta PuHP_{l,t}^{Ge}$ and $\Delta PuHP_{l,t}^{Pu}$ are the violated interval of the generation and pumping power of the PuHP. $\Delta ThPP_{1,t}^{Ge}$ is the violated interval of the first ThPP. $\Delta V_{l,t}$ is the violated interval of the volume of the PuHP.

4. NUMERICAL RESULTS

The study implements two metaheuristic algorithms, including EO and SBOA, to solve the optimal generation problem for hybrid power systems. EO and

SBOA are programmed on the Matlab software with the 2019A version and run on an 8-GB RAM and 2.4 GHz processor computer.

4.1 The Simulation Results for System 1

System 1 comprises two ThPPs and one SoPPs. Data from the two ThPPs are taken from [4] and shown in Table 1. The solar radiations are taken from Khanh Hoa

province, Vietnam, at the geography coordinates 11.696676°, 109.019531° and the rated power of SoPP is 450MW [29]. The system is plotted in Figure 3. The power demand of loads and the hourly generation of SoPP are plotted in Figure 4. To implement the two algorithms, the population and iteration number are set to 50 and 250 for EO and 25 and 250 for SBOA.

Table 1. Fuel cost function and generation limits of two ThPPs

| k | a_k | b_k | c_k | $ThPP_{k}^{Ge,Min}$ (MW) | $ThPP_k^{Ge,Max}$ (MW) |
|---|---------|--------|-------|--------------------------|------------------------|
| 1 | 3,877.5 | 3.9795 | 0.08 | 10 | 2,500 |
| 2 | 3,900 | 3.9 | 0.081 | 10 | 2,500 |

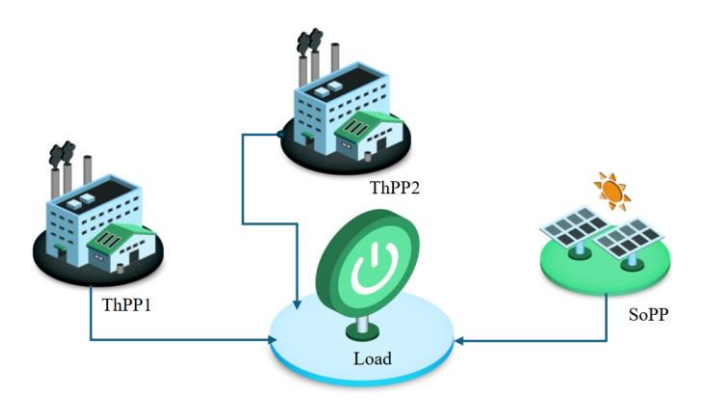


Fig. 3. The typical configuration of System 1.

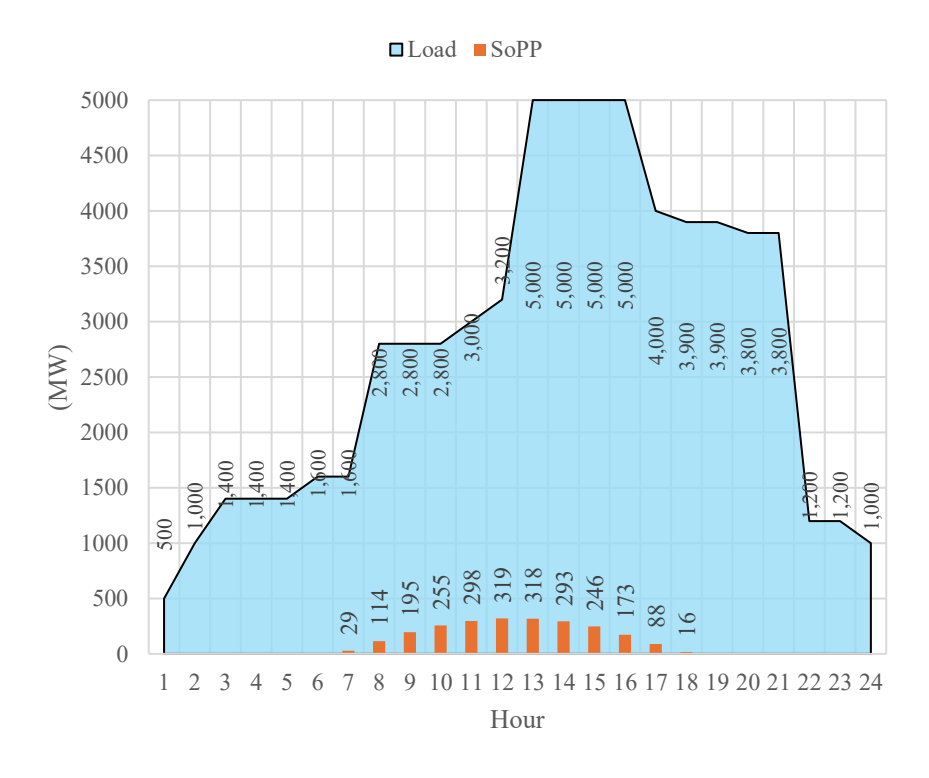


Fig. 4. Load demand and solar photovoltaic power plant's generation.

A summary of the total fuel cost of the two ThPPs is plotted in Figure 5. The best total cost is \$9,155,384.3, obtained by EO; meanwhile, SBOA's total cost is \$9,155,387.3. The fluctuation of EO is smaller than that of SBOA. The box height of EO is lower than that of SBOA. In addition, the middle and the peak of EO are

\$9,155,388.5 and \$9,155,411.5, whereas they are \$9,155,407.2 and \$9,155,480.4 for SBOA. The boxplot reveals that EO has better or more stable performance than SBOA. Figures 6 and 7 show the search process of the best run and the mean of all fifty runs. In the best runs, EO converged to the global optimal solution at the

200th iteration, and the improvement of the solution from the 201th to the 250th iterations is not clearly seen. On the contrary, SBOA cannot converge to the best solution at the last iteration. In the mean curve of all fifty runs, the fitness functions of EO seem not to change from the

200th to the last iterations, but those of SBOA are decreased significantly from the 200th to the last iterations. The convergence characteristics confirm that EO is much faster and more stable than SBOA for fifty runs.

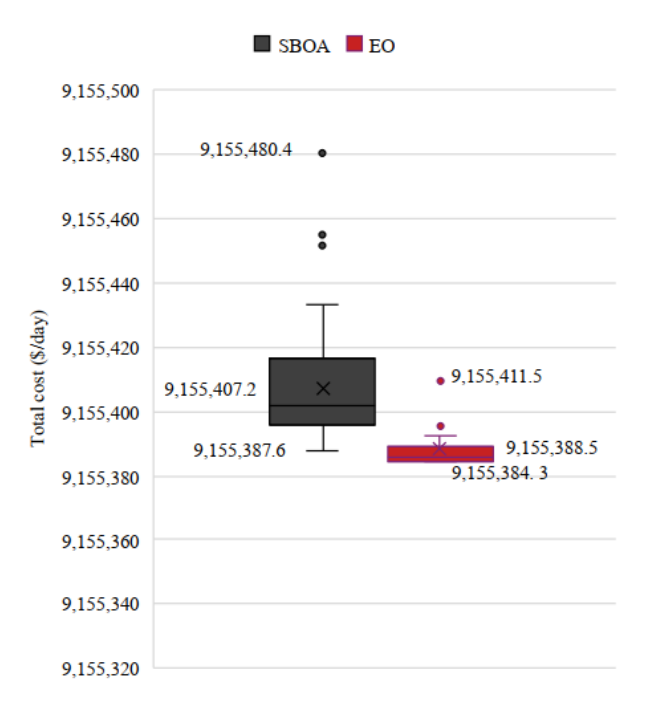


Fig. 5. Summary of results obtained by EO and SBOA.

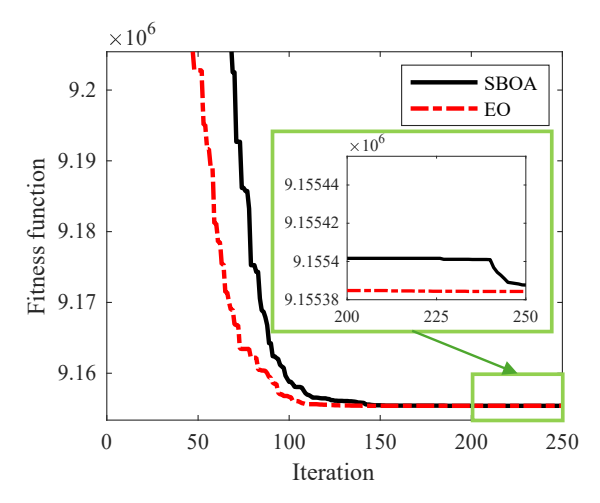


Fig. 6. The search process of the best run.

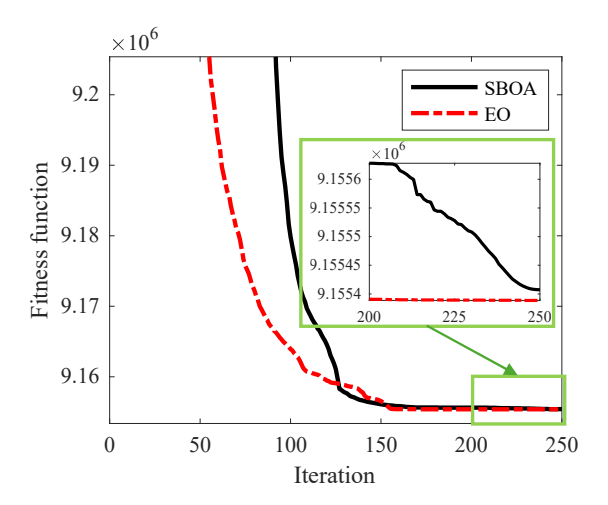


Fig. 7. The mean search process of all fifty runs.

To investigate the search performance for the system, the population and iteration numbers increased from 50 and 250 to 100 and 400 for EO, and from 25 and 250 to 50 and 400 for SBOA. The summary of results is shown in Figure 8. The results show that the performance of SBOA and EO has improved. EO can

find many of the best solutions, and SBOA can find the same solution. The difference between the fifty solutions obtained by EO is tiny, and the best total cost for this system is \$9,155,384.02. Figure 9 and 10 indicate that EO is faster and more stable than SBOA, and the difference is clear after the 300th iteration.

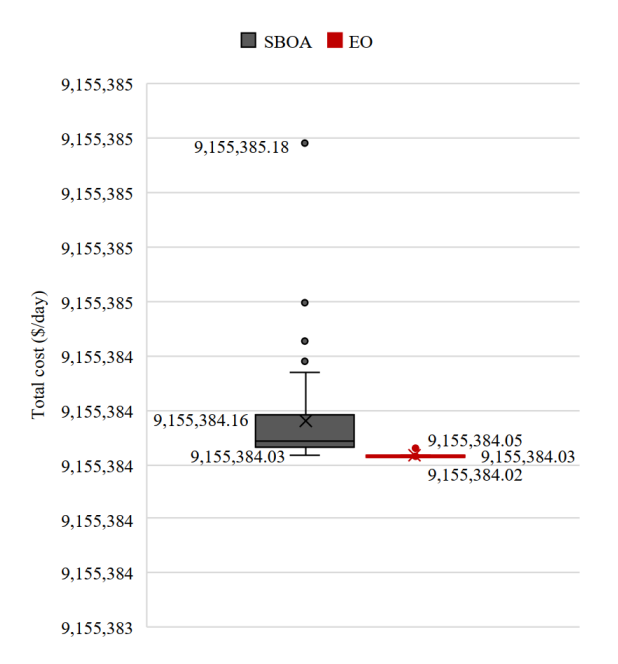


Fig. 8. Summary of results obtained by EO and SBOA after increasing control parameters.

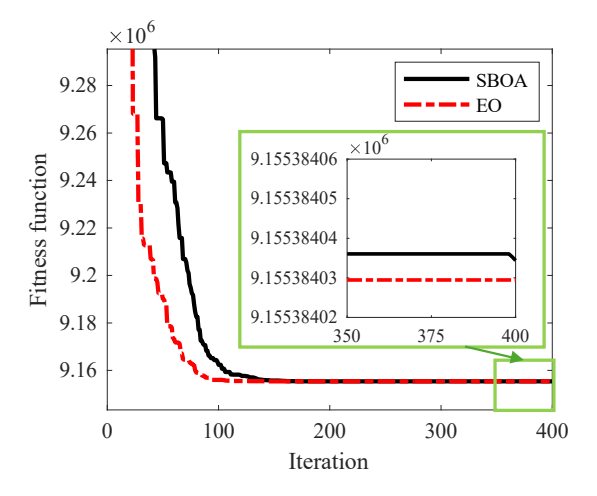


Fig. 9. The search process of the best run after increasing control parameters.

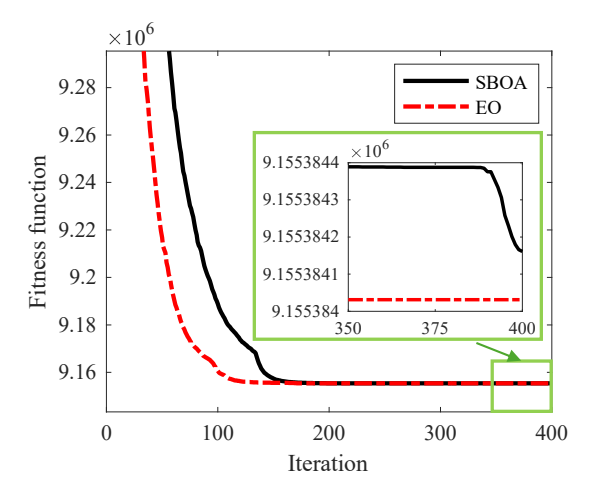


Fig. 10. The mean search process of all fifty runs after increasing control parameters.

4.2 The Simulation Results for System 2

System 2 has two ThPPs, one SoPP, and one PuHP, and its configuration is plotted in Figure 11. To show the value of pumps in water storage function, the system is simulated under two cases as follows:

Case 1: The PuHP does not run pumps for the whole schedule

Case 2: The PuHPs runs pumps for water storage. To have a high possibility of finding the most effective solution for the system, the population and iteration number are set to 100 and 1,000 for EO and 50 and 1,000 for SBOA. Figure 12 and Figure 13 summarize the total cost of fifty runs for Case 1 and Case 2. EO can find better solutions than SBOA for the two cases. The

best cost of EO is \$9,087,475.0 for Case 1 and \$9,006,450.4 for Case 2; meanwhile, those are \$9,087,482.3 and \$9,010,754.6 for SBOA. For Case 1, EO has very tiny fluctuations since the best, mean, and maximum values are approximately the same, around \$9,087,475.0 SBOA fluctuates very high since the difference between the smallest and highest values is very high. EO in Case 2 is not as good as in Case 1 since the fluctuations are much higher. SBOA still has much higher fluctuations than EO because its minimum and maximum values have a very high deviation. So, it can be concluded that EO is more suited to the problem than SBOA.



Fig. 11. The typical configuration of System 2 for case 2.

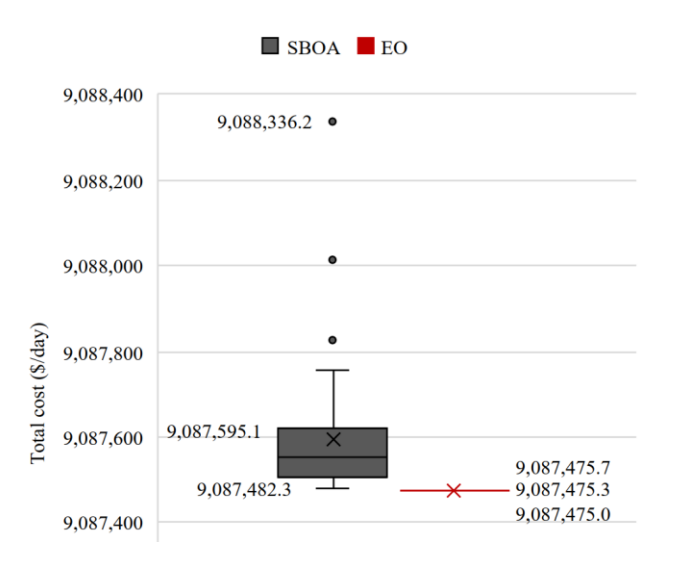


Fig. 12. Summary of results for Case 1 of System 2.

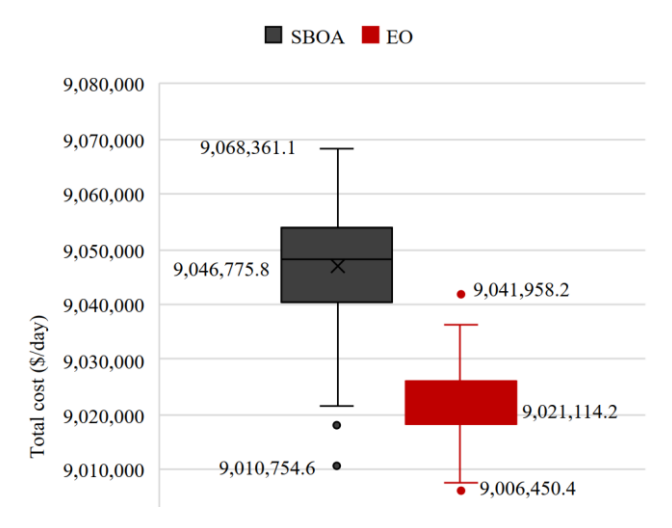


Fig. 13. Summary of results for Case 2 of System 2.

4.3 Discussion on the Study Cases

The total cost of one day is compared in Figure 14 for the two systems. System 1, without the operation of PuHP, paid the highest cost of \$9,155,384 whereas System 2, with the operations of pumps, paid the smallest total cost of \$9,006,450. System 2, without the operation of pumps, paid a smaller total cost than

System 1 by \$67,909.7, about 0.79%, but it reached a higher total cost than System 2 with the operation of pumps. Using the pumps in PuHP makes the total cost smaller than System 1 by \$148,934, and System 2 without the pump operation costs \$81,025 per day. The total cost reduction is about 1.63% and 0.9% of the total cost from System 1 and System 2 without running pumps.

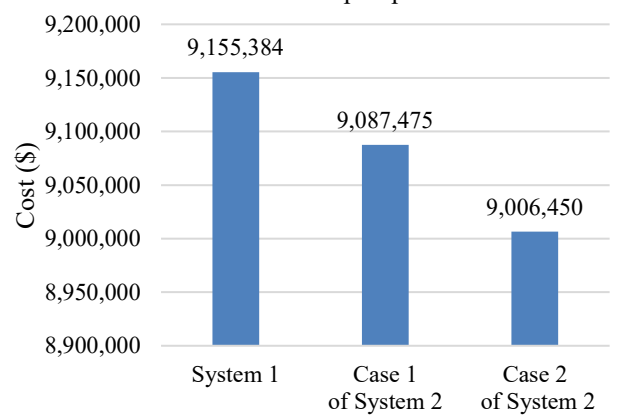


Fig. 14. Comparison of total costs among study cases.

To clarify why Case 1 of System 2 can pay less than System 1, and Case 2 of System 2 can pay less than Case 1 of System 2, Figures 15 and 16 are plotted. The hourly cost of the two ThPPs and the reduced cost are presented in the figures. The reduced cost is obtained by using the following calculation: System 1 minus Case 1 of System 2, and Case 1 of System 2 minus Case 2 of System 2. Figure 15 indicates that System 1 and Case 1 of System 2 have the same hourly cost for hours excluding three hours 14–16, so the reduced cost of the hours is zero, but the cost of hours 14–16 is high. These reduced costs are \$3,167, \$22,055 and \$42,688,

respectively, and the sum of the reduced costs is about \$67,910. In Figure 16, the reduced costs are negative for five hours (1–4 and 6), zero for fifteen hours (5–12, 16–17, and 19–24), and positive for four hours (13–15 and 18). The negative reduced costs are -\$5,317.7, -\$9,766.7, -\$13,135.5, -\$13,028.7, and -\$547.6, and their sum is -41796.2. The positive reduced costs are \$41,301.8, \$38,020.9, \$18,056.3, \$25441.8, and their sum is 122,820.9. The sum of negative and positive reduced costs is equal to (\$122,820.9 - \$41,796.2) = \$81,024.7. The value 81,024.7 is also the saving cost of Case 2 compared to Case 1 of System 2.

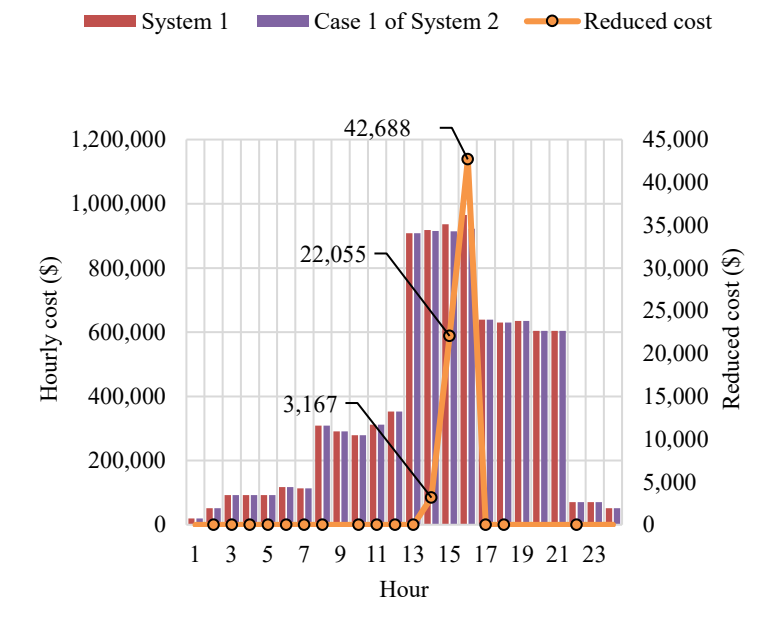


Fig. 15. The hourly cost comparison of ThPPs in System 1 and Case 1 of System 2.

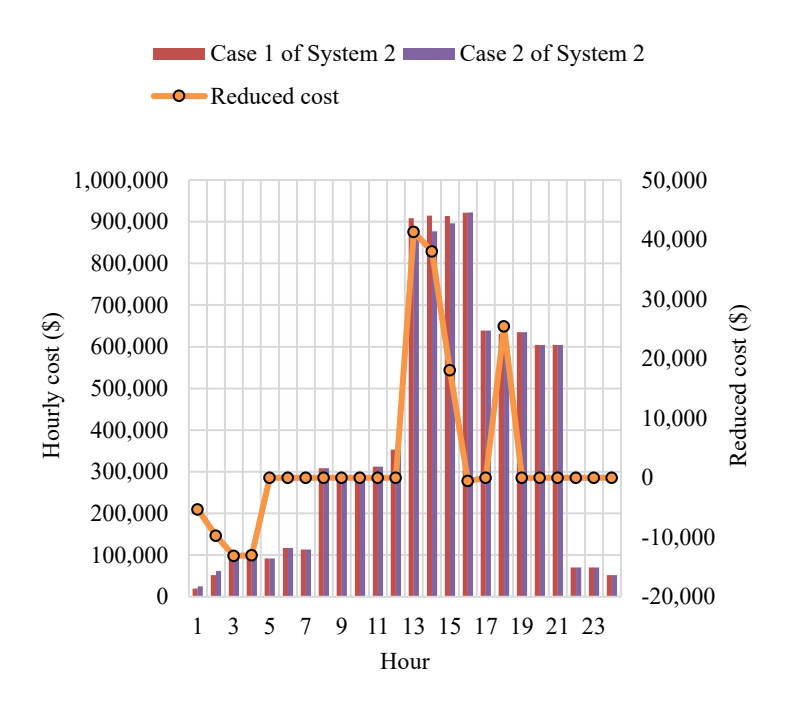


Fig. 16. The hourly cost comparison of ThPPs in Cases 1 and 2 of System 2.

Figure 17 compares the optimal generation in System 1 and System 2 without running the pumps of PuHP. The load demand is supplied enough by the total generation of two ThPPs and one SoPP in Figure 17a and by the total generation of two ThPPs, one SoPP, and one PuHP in Figure 17b. So, the difference is that System 2 has more generations from the PuHP. All the power plants satisfy the generation limitations. There is

a tiny difference between the two subfigures in the generation of PuHP at hours 14–16. The generation of PuHP is very small at hour 14 and increases at hour 15 and hour 16. The generation of the PuHP is 8.27, 57.389, and 110 MW at these hours. So, the total cost of System 2 without running the pumps of PuHP is much smaller than that of System 1.

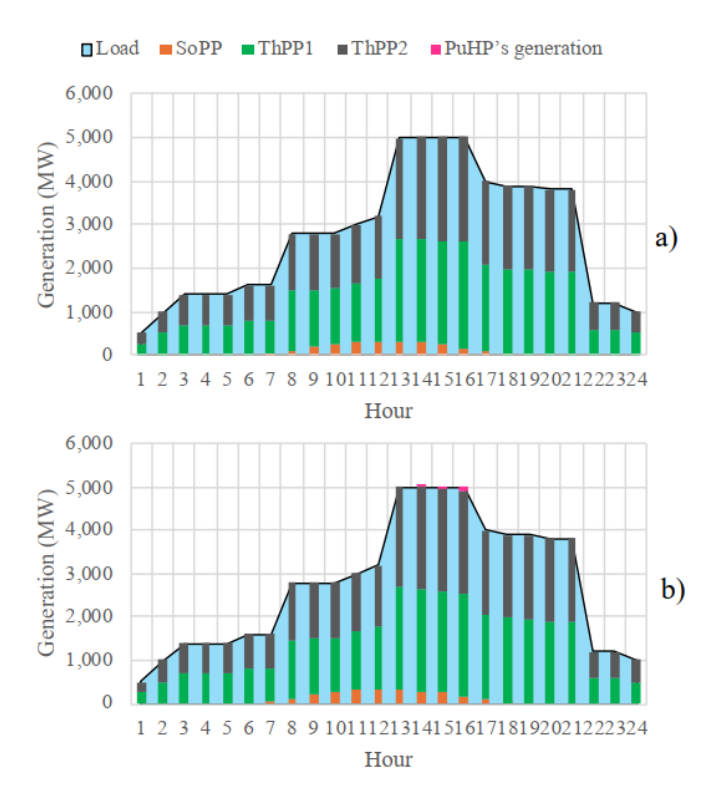


Fig. 17. Comparison of optimal generations: a) System 1 and b) Case 1 of System 2.

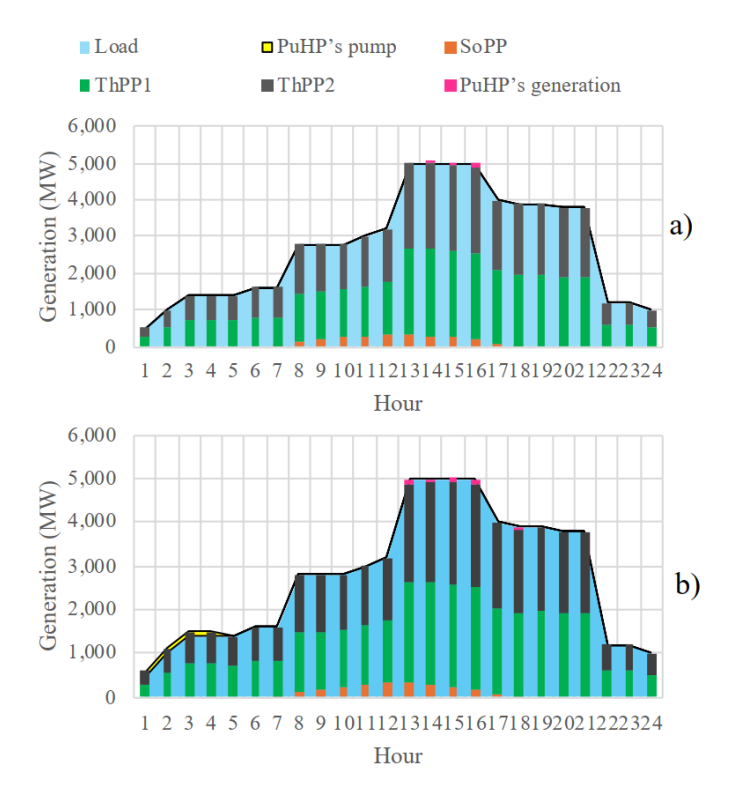


Fig. 18. Comparison of optimal generation in System 2: a) Case 1 of System 2 b) Case 2 of System 2.

A comparison of optimal generation in System 2 without and with running pumps of PuHP is shown in Figure 18. The two figures have two differences, which are comprised of the number of hours of generating and pumping. Firstly, Figure 18a shows three hours 14–16 with generation, while Figure 18b shows five hours 13–16 and 18 with generation. Secondly, Figure 17b has five hours of 1–5 running pumps, while Figure 17a shows none of the hours running pumps. In detail, the

generation is respectively 8.27, 57.389, and 110 MW in Figure 18a, and 109.726, 108.921, 104.905, 108.677, and 81.205 MW in Figure 18b. The total generated energy is 175.667 MWh in Figure 17a and 513.433 MWh in Figure 17b. The pumping power is 109.180, 108.986, 107.451, and 106.494 MW, as shown in Figure 18b. The total consumed energy by pumps is 432.111 MWh in Figure 17b. So, if we compare the effectiveness of energy, Case 2 only produces (513.433 - 432.111) =

81.322 MWh, which is smaller than 175.667 MWh in Case 1 by 94.345 MWh.

Figure 19 reports the hydraulic parameters of the PuHP for one operating day. The two subfigures have the same values of inflows and different values of other parameters, such as discharges, volumes, and storage. Figure 19a does not have storage because the system did not run pumps; meanwhile, we can see the parameter in Figure 19b. The volume starts and ends at the same value of 1594×10^6 m³ in the two subfigures. This means that the two study cases satisfy the initial and final volume constraints. Case 1 has three hours with discharge; meanwhile, Case 2 has five hours with discharge. The difference is because Case 2 runs pumps at hours 1–4. The volume in Case 2 is also higher than

in Case 1. The total inflow of 24 hours is 316 m3/s in two cases. The total discharge is 316 m3/s in Case 1, but it is 923.523 m3/s in Case 2. The total storage is 607.523 in Case 2. It is correct that the total discharge in Case 2 is the sum of the total inflow and the total storage, which is (316 + 607.523) = 923.523 m3/s. Thanks to the pumping function, Case 2 has a greater amount of water than Case 1 to produce electricity. The total generated energy in Case 1 is 175.667 MWh, while that is 513.433 MWh in Case 2. However, Case 2 used 432.111 MWh to run pumps. So, if we compare the effectiveness of energy, Case 2 only produces (513.433 - 432.111) = 81.322 MWh, which is smaller than 175.667 MWh in Case 1 by 94.345 MWh.

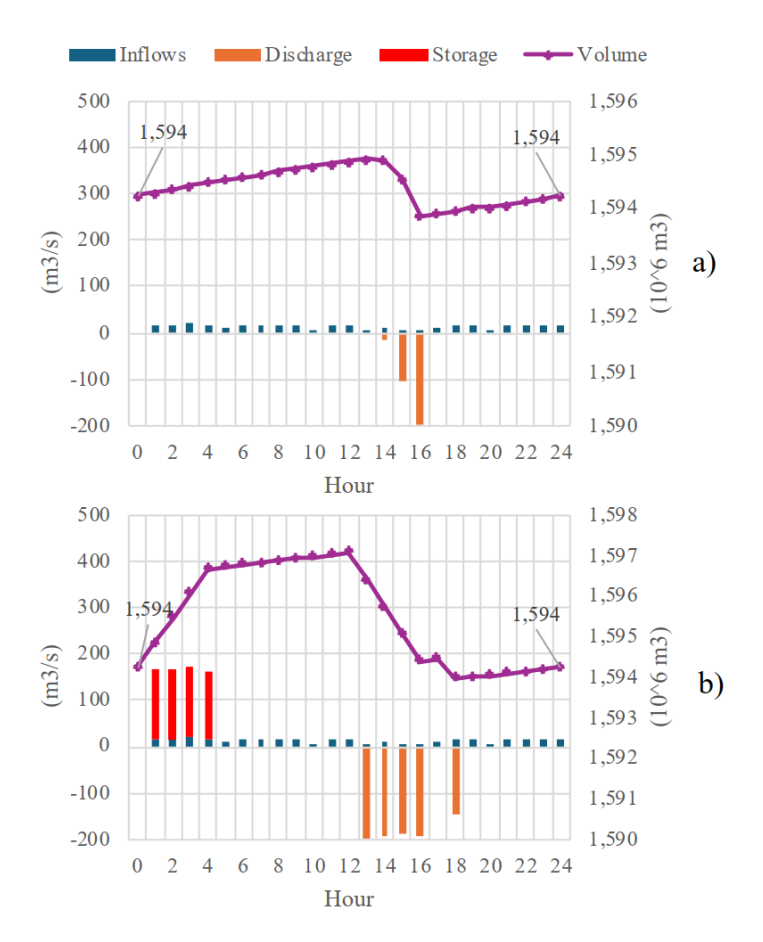


Fig. 19. Hydraulic parameters of Case 2 of System 2.

5. CONCLUSIONS

In this study, the EO and SBOA were successfully employed to optimize power generation allocation within hybrid power systems that incorporate renewable power plants. The primary objective is to minimize the total fossil fuel costs associated with electricity generation from ThPPs. Both EO and SBOA were applied to optimize the operational parameters of ThPPs and PuHPs simultaneously over 24 periods. The study has considered the variable pump speed for the PuHPs for flexible water storage. This optimization was conducted for two different power system configurations and different cases as follows:

1) System 1 was comprised of two ThPPs and one SoPP

2) System 2 was the integration of one more PuHP into System 1. Two simulation cases were performed for the system: Case 1-the PuHP worked as a conventional plant without running its pumps for water storage, and Case 2-the PuHP could run pumps for water storage.

After running EO and SBOA for the study cases with different settings of control parameters, the results are as follows:

1) EO and SBOA reached the best cost of \$9,155,384.263 and \$9,155,387.624 for System 1, \$9,087,475.0 and \$9,087,482.3 for Case 1 of System 2, and \$9,006,450.4 and \$9,010,754.6 for Case 2 of System 2. So, EO found a lower cost than SBOA by \$3.361, \$7.3, and \$4,304.2

- for System 1, Cases 1 and 2 of System 2, respectively. Clearly, EO and SBOA had approximately the same good optimization operation solutions for simple systems without PuHP or with PuHP, but neglecting the another pumping function. For more complicated system with PuHP and consideration of pumping functions, EO outperformed SBOA clearly.
- 2) System 1 paid \$9,155,384, whereas Cases 1 and 2 of System 2, respectively, paid \$9,087,475.0 and \$9,006,450 for the total fuel cost of ThPPs. So, Case 2 of System 2 could pay less money than System 1 and Case 1 of System 2 by \$148,934 and \$81,025, corresponding to 1.63% and 0.9%. The results indicated that the presence of the PuHP in hybrid power systems is very beneficial in reducing the cost of fossil fuels in ThPPs.

Besides the results and achievements mentioned above, the study still has several shortcomings that need to be improved for better quality as follows: 1) all the parameters of the mentioned power systems are not the actual parameters of the real system; 2) the consideration of only 24 periods for an operational day is conservative compared to the real operational situation; 3) the effect of electricity price in both selling and buying is not evaluated, *etc*. To remove all these limitations, future work should be conducted in the real power system, considering the large operational schedule, and lastly, the effect of the electricity market must be considered and analyzed to clearly demonstrate the benefit of operating PuHPs in the long term

REFERENCES

- [1] Mohammadi F., Sanjari M. and Saif M., 2022. A real-time blockchain-based state estimation system for battery energy storage systems. In 2022 IEEE Kansas Power and Energy Conference (KPEC), IEEE, pp: 1–4.
- [2] Abdi H., Mohammadi-ivatloo B., Javadi S., Khodaei A.R., and Dehnavi E., 2017. Energy storage systems. *Distributed Generation Systems*7: 333–368.
- [3] Muruganantham B., Gnanadass R. and Padhy N.P., 2017. Challenges with renewable energy sources and storage in practical distribution systems. *Renewable and Sustainable Energy Reviews* 73: 125–134.
- [4] Ha P.T., Dinh B.H., Phan T.M. and Nguyen T.T., 2024. Jellyfish search algorithm for optimization operation of hybrid pumped storage-wind-thermal-solar photovoltaic systems. *Heliyon* 10(7): e29339.
- [5] Ha P.T., Tran D.T., Phan T.M., and Nguyen T.T., 2024. Maximization of total profit for hybrid hydro-thermal-wind-solar power systems considering pumped storage, cascaded systems, and renewable energy uncertainty in a real zone, Vietnam. *Sustainability*, 16(15): 6581.

- [6] Özyön S., 2020. Optimal short-term operation of pumped-storage power plants with differential evolution algorithm. *Energy* 194: 116866.
- [7] Shi L., Yang F., Li Y., Zheng T., Wu F. and Lee K.Y., 2022. Optimal configuration of electrochemical energy storage for renewable energy accommodation based on operation strategy of pumped storage hydro. *Sustainability* 14(15): 9713.
- [8] Phan T.M. and T. Trong Dao, 2024. Self-organizing migrating algorithm (SOMA) for pumped-storage hydrothermal system scheduling. In *International Conference on Advanced Engineering Theory and Applications*, Ho Chi Minh City, Vietnam; 8-10 December; Springer, Singapore. Pages: 475–485.
- [9] Tran D.T. and T.M. Phan. 2024. Minimize total cost and maximize total profit for power systems with pumped storage hydro and renewable power plants using improved self-organizing migration algorithm. *Journal of Engineering and Technological Sciences* 56(1): 81–94.
- [10] Alvarez G.E., 2020. Operation of pumped storage hydropower plants through optimization for power systems. *Energy* 202: 117797.
- [11] Alturki F.A. and E.M. Awwad. 2021. Sizing and cost minimization of standalone hybrid WT/PV/biomass/pump-hydro storage-based energy systems. *Energies*, 14(2): 489.
- [12] Singh N.K., Koley C., Gope S., Dawn S. and Ustun T.S., 2021. An economic risk analysis in wind and pumped hydro energy storage integrated power system using meta-heuristic algorithm. *Sustainability* 13(24): 13542.
- [13] Kiene S. and O. Linkevics. 2021. Simplified model for evaluation of hydropower plant conversion into pumped storage hydropower plant. *Latvian Journal of Physics and Technical Sciences* 58(3): 108–120.
- [14] Kumar R. and A. Kumar, 2025. Optimal scheduling of variable speed pumped storage, solar and wind energy system. *Energy Sources, Part A: Recovery, Utilization, and Environmental Effects*, 47(1): 5225–5239.
- [15] Ahmadi S., Tostado-Véliz M., Ghadimi A.A., Miveh M.R. and Jurado F., 2022. A novel interval-based formulation for optimal scheduling of microgrids with pumped-hydro and battery energy storage under uncertainty. *International Journal of Energy Research* 46(9): 12854–12870.
- [16] Makhdoomi S. and A. Askarzadeh. 2023. Techno-enviro-economic feasibility assessment of an off-grid hybrid energy system with/without solar tracker considering pumped hydro storage and battery. *IET Renewable Power Generation*, 17(5): 1194–1211.
- [17] Menesy A.S., Sultan H.M., Habiballah I.O., Masrur H., Khan K.R. and Khalid M., 2023. Optimal configuration of a hybrid photovoltaic/wind turbine/biomass/hydro-pumped storage-based energy system using a heap-based optimization algorithm. *Energies* 16(9): 3648.

- [18] Amoussou I., Tanyi E., Ali A., Agajie T.F., Khan B., Ballester J.B. and Nsanyuy W.B., 2023. Optimal modeling and feasibility analysis of gridinterfaced solar pv/wind/pumped hydro energy storage based hybrid system. *Sustainability*, 15(2): 1222.
- [19] Kumar R. and A. Kumar. 2025. Optimal scheduling for solar wind and pumped storage systems considering imbalance penalty. *Energy Sources, Part A: Recovery, Utilization, and Environmental Effects*, 47(1): 2584–2595.
- [20] Fan H., Wu H., Li S., Han S., Ren J., Huang S. and Zou H., 2025. Optimal scheduling method of combined wind–photovoltaic–pumped storage system based on improved bat algorithm. *Processes* 13(1): 101.
- [21] Tardy A., Rousse D.R., Mungyeko Bisulandu B.-J.R. and Ilinca A., 2025. Enhancing energy sustainability in remote mining operations through wind and pumped-hydro storage; application to Raglan Mine, Canada. *Energies* 18(9): 2184.
- [22] Kharrich M., Kamel S., Abdeen M., Mohammed O.H., Akherraz M., Khurshaid T. and Rhee S.-B., 2021. Developed approach based on equilibrium optimizer for optimal design of hybrid pv/wind/diesel/battery microgrid in Dakhla, Morocco. *IEEE Access* 9: 13655–13670.
- [23] Kharrich M., Abualigah L., Kamel S., AbdEl-Sattar H. and Tostado-Véliz M., 2022. An improved arithmetic optimization algorithm for design of a microgrid with energy storage system:

- case study of El Kharga Oasis, Egypt. *Journal of Energy Storage* 51: 104343.
- [24] Kharrich M., Selim A., Kamel S. and Kim J., 2023. An effective design of hybrid renewable energy system using an improved Archimedes Optimization Algorithm: A case study of Farafra, Egypt. *Energy Conversion and Management* 283: 116907.
- [25] Faramarzi A., Heidarinejad M., Stephens B. and Mirjalili S., 2020. Equilibrium optimizer: A novel optimization algorithm. *Knowledge-Based Systems*, 191: 105190.
- [26] Fu Y., Liu D., Chen J. and He L., 2024. Secretary bird optimization algorithm: a new metaheuristic for solving global optimization problems. *Artificial Intelligence Review* 57(5): 123.
- [27] Zhu Y., Zhang M., Huang Q., Wu X., Wan L. and Huang J., 2025. Secretary bird optimization algorithm based on quantum computing and multiple strategies improvement for KELM diabetes classification. *Scientific Reports* 15(1): 3774.
- [28] Tu F., Zheng S. and Chen K., 2025. Optimal active-reactive power dispatch for distribution network with carbon trading based on improved multi-objective equilibrium optimizer algorithm. *IEEE Access* 13: 18899–18911.
- [29] The Global Solar Atlas. Solar radiations. [Online], Retrieved March 15, 2025 from the World Wide Web: https://globalsolaratlas.info/map